Pinkard, R. N., & Weir, D. M. (1978) in *Handbook of Experimental Immunology* (Weir, D. M., Ed.) Chapter 16, pp 16.1–16.20, Blackwell Scientific, Oxford.
Pollack, S. E., & Auld, D. S. (1982) *Anal. Biochem. 127*, 81–88.
Richards, F. M. (1958) *Proc. Natl. Acad. Sci. U.S.A. 44*, 162–166.
Richards, F. M., & Vithayathil, P. J. (1959) *J. Biol. Chem. 234*, 1459–1465.
Riordan, J. F., & Livingston, D. M. (1971) *Biochem. Biophys. Res. Commun. 44*, 695–701.
Rupley, J. A. (1967) *Methods Enzymol. 11*, 905–917.
Solomon, B., Koppel, R., Kenett, D., & Fleminger, G. (1989) *Biochemistry 28*, 1235–1241.
Strydom, D. J., Fett, J. W., Lobb, R. R., Alderman, E. M., Bethune, J. L., Riordan, J. F., & Vallee, B. L. (1985) *Biochemistry 24*, 5846–5494.
Vallee, B. L., & Riordan, J. F. (1968) *Brookhaven Symp. Biol. 21*, 91–119.
Vallee, B. L., Galdes, A., Auld, D. S., & Riordan, J. F. (1983) in *Metal Ions in Biology* (Spiro, T. G., Ed.) Vol. 5, pp 25–75, Wiley, New York.
Vita, C., Dalzoppo, D., & Fontana, A. (1985) *Biochemistry 24*, 1798–1806.

# Mechanism for Activation of the 4-Nitrobenzo-2-oxa-1,3-diazole-Labeled Sarcoplasmic Reticulum ATPase by $Ca^{2+}$ and Its Modulation by Nucleotides†

Shigeo Wakabayashi and Munekazu Shigekawa*
*Department of Molecular Physiology, National Cardiovascular Center Research Institute, Suita, Osaka 565, Japan*
*Received January 3, 1990; Revised Manuscript Received April 25, 1990*

ABSTRACT: The mechanism for activation of sarcoplasmic reticulum ATPase by $Ca^{2+}$ was investigated in 2 mM $MgCl_2$ and 0.1 M KCl at pH 6.5 and 11 °C by using enzyme preparations in which a specific amino acid residue (Cys-344) was labeled with 4-nitrobenzo-2-oxa-1,3-diazole (NBD) [Wakabayashi, S., Imagawa, T., & Shigekawa, M. (1990) *J. Biochem. (Tokyo) 107*, 563–571]. We compared the kinetics of binding and dissociation of $Ca^{2+}$ from the enzyme with those of the accompanying NBD fluorescence changes. The fluorescence rise following addition of $Ca^{2+}$ proceeded monoexponentially. At 2–100 μM $Ca^{2+}$ and in the absence of nucleotides, the $Ca^{2+}$-induced fluorescence rise and $Ca^{2+}$ binding to the enzyme proceeded at similar rates, which were almost independent of the $Ca^{2+}$ concentration. In contrast, the fluorescence decrease induced by $Ca^{2+}$ removal was slower than the $Ca^{2+}$ dissociation, and both of these processes were inhibited markedly by increasing medium $Ca^{2+}$. ATP by binding at 1 mol/mol of the phosphorylation site markedly accelerated both the $Ca^{2+}$-induced fluorescence rise and $Ca^{2+}$ binding, ADP and AMPPNP but not GTP also being effective. In contrast, ADP minimally affected the NBD fluorescence decrease and the $Ca^{2+}$ dissociation. These data are consistent with a reaction model in which binding of $Ca^{2+}$ occurs after the conformational transition of the free enzyme from a state ($E_2$) having low affinity for $Ca^{2+}$ to one ($E_1$) having high affinity for $Ca^{2+}$ and in which ATP bound at the catalytic site of $E_2$, whose affinity for ATP is about 30-fold less than that of $E_1$, accelerates this conformational transition.

It is well established that the sarcoplasmic reticulum (SR)[1] $Ca^{2+}$-ATPase is activated by binding of two moles of $Ca^{2+}$ to its high-affinity sites (de Meis & Vianna, 1979; Martonosi & Beeler, 1983). This $Ca^{2+}$ binding is accompanied by a change in the enzyme conformation, which has been detected by changes in the spectral parameters (Inesi et al., 1980; Dupont & Leigh, 1978; Guillain et al., 1980, 1981; Pick & Karlish, 1980), in tryptic digestion patterns (Imamura et al., 1984; Andersen et al., 1985), and in reactivity of amino acid residues of the enzyme (Ikemoto et al., 1978; Murphy, 1978). This $Ca^{2+}$-induced conformational transition in the $Ca^{2+}$-ATPase has been shown to be influenced by changes in the experimental conditions such as pH and presence or absence of ATP and/or $Mg^{2+}$ (Inesi et al., 1980; Guillain et al., 1980, 1982; Scofano et al., 1979; Pick & Karlish, 1982; Champeil et al., 1983; Froud & Lee, 1986).

The transient kinetics of ATPase activation by $Ca^{2+}$ have been studied by following enzyme phosphorylation by ATP or $P_i$ (Guillain et al., 1981; Scofano et al., 1979; Sumida et al., 1978; Petithory & Jencks, 1988a,b), a change in the intrinsic fluorescence of the ATPase (Dupont & Leigh, 1978; Guillain et al., 1980; Champeil et al., 1983; Dupont, 1982; Fernandez et al., 1984) and direct binding of radioactive calcium to the enzyme (Dupont, 1982, 1984). The data obtained in these studies showed that $Ca^{2+}$ binding is a complex, multistep process involving enzyme isomerization. According to these and other data (Ikemoto et al., 1981; Inesi, 1987), the two calcium sites on the enzyme are not kinetically identical, and binding and release of $Ca^{2+}$ follow an ordered process.

According to the "$E_1$–$E_2$" (or E–E*) model for the $Ca^{2+}$-ATPase (de Meis & Vianna, 1979), which has been widely used to explain the experimental results, the enzyme activation involves $Ca^{2+}$-induced transition of the enzyme conformation

†This work was supported by Grant-in-Aid for Scientific Research on Priority Areas (62617524) from the Ministry of Education, Science and Culture of Japan.

[1] Abbreviations: SR, sarcoplasmic reticulum; FITC, fluorescein 5′-isothiocyanate; NBD-Cl, 7-chloro-4-nitrobenzo-2-oxa-1,3-diazole; AMPPNP, adenosine 5′-(β,γ-imino)triphosphate; EGTA, ethylene glycol bis(β-aminoethyl ether)-*N*,*N*,*N*′,*N*′-tetraacetic acid; Mes, 2-(*N*-morpholino)ethanesulfonic acid; Mops, 3-(*N*-morpholino)propanesulfonic acid; EDANS, *N*-acetyl-*N*′-(5-sulfo-1-naphthyl)ethylenediamine.

0006-2960/90/0429-7309$02.50/0 

from the inorganic phosphate reactive form ($E_2$) to the ATP-reactive form ($E_1$). This conformational transition is considered to be accompanied by changes in the sidedness and affinity of the calcium sites. This two-site model, however, cannot readily explain some of the previous data. For example, measurements of the intrinsic protein fluorescence change (Champeil et al., 1983) and of enzyme phosphorylation by [$\gamma$-$^{32}$P]ATP and internalization of $^{45}Ca^{2+}$ (Petithory & Jencks, 1988b) revealed that both fast and slow binding of $Ca^{2+}$ to the enzyme occurred at pH 7 and 20–25 °C in millimolar $Mg^{2+}$. To explain these complex kinetics of $Ca^{2+}$ binding, several elaborate reaction mechanisms have been proposed (Champeil et al., 1983; Petithory & Jencks, 1988b; Dupont, 1982; Fernadez et al., 1984). None of these mechanisms, however, can be considered to be established, because sufficient information is still not available concerning the transient kinetics of $Ca^{2+}$ binding to the enzyme, the accompanying changes in the enzyme conformation, and the mechanisms for the effects of ligands such as ATP, $Mg^{2+}$, and $H^+$ on these processes.

Fluorescence probes have been useful in monitoring rapid conformational transitions. However, appropriate probes other than the intrinsic protein fluorescence have not so far been used to monitor rapid changes in the conformation of the unphosphorylated form of the $Ca^{2+}$-ATPase. Because of this, we are not certain even as to what the intrinsic fluorescence signal monitors in the enzyme: the intrinsic fluorescence could monitor major conformational transitions such as the putative $E_1$–$E_2$ conformational transition (de Meis & Vianna, 1979) or simply the local occupancy of the $Ca^{2+}$ sites. It is therefore highly desirable to obtain new well-characterized fluorescence probes whose signals can monitor the $Ca^{2+}$-induced conformational transition.

In our previous paper (Wakabayashi et al., 1990), we reported successful incorporation of a fluorescent NBD label into a specific sulfhydryl residue (Cys-344) near the phosphorylation site of the $Ca^{2+}$-ATPase. We found that $Ca^{2+}$ binding to the enzyme induced up to a 2-fold increase in the intensity of the NBD fluorescence and that the $Ca^{2+}$ binding and the NBD fluorescence exhibited the same $Ca^{2+}$ concentration dependence under equilibrium conditions. Furthermore, we found that at low pH (6.0) the enzyme states could be grouped into two categories, one being in a high-fluorescence state (the unphosphorylated enzyme with bound calcium, the enzyme–ATP–calcium complex, and the ADP-sensitive phosphoenzyme) and the other being in a low-fluorescence state (the unphosphorylated enzyme without bound calcium, the ADP-insensitive phosphoenzyme, and the enzyme–vanadate complex). This behavior of NBD fluorescence is seemingly compatible with the $E_1$–$E_2$ model of $Ca^{2+}$-ATPase (de Meis & Vianna, 1979), in which two major conformations of enzyme are assumed to alternate during enzyme turnover.

In this study, using the fluorescence signal of the NBD label incorporated into the $Ca^{2+}$-ATPase, we compare directly the time courses of the $Ca^{2+}$-induced changes in the enzyme conformation with those for the binding and release of $Ca^{2+}$ from the NBD-labeled enzyme. Our aims are (i) to clarify the relationship between $Ca^{2+}$ binding and the enzyme conformational change and (ii) to study the mechanism by which ATP accelerates this $Ca^{2+}$-induced conformational transition.

## Experimental Procedures

*Preparation of SR $Ca^{2+}$-ATPase.* Leaky, purified $Ca^{2+}$-ATPase vesicles were prepared from SR membranes isolated from rabbit white skeletal muscle (Shigekawa et al., 1983). The ATPase prepartion was finally suspended in 0.1 M KCl, 0.3 M sucrose, and 10 mM histidine solution (pH 6.8) and stored at −80 °C.

*Modification of $Ca^{2+}$-ATPase with NBD-Cl.* The modification of $Ca^{2+}$-ATPase with NBD-Cl was performed as described elsewhere in detail (Wakabayashi et al., 1990). Briefly, the purified ATPase (2 mg/mL) was incubated at 25 °C in the dark for 60 min with 0.3 mM NBD-Cl in 0.2 M KCl, 13 mM Mops/KOH (pH 7.0), 1 mM AMPPNP, and 1 mM $CaCl_2$. The labeling reaction was terminated by adding at least 4 volumes of ice-cold KCl–sucrose–histidine solution, and excess NBD-Cl was subsequently removed by centrifuging the mixture at 70000*g* for 30 min. The resulting pellet was suspended in the same KCl–sucrose–histidine solution. The NBD-labeled enzyme (3–4 mg/mL) was treated further in the dark at 25 °C for 7 min with the KCl–sucrose–histidine solution containing 10 mM DTT, 1 mM $CaCl_2$, and 0.5 mM AMPPNP. The DTT treatment was stopped by adding at least 8 volumes of ice-cold KCl–sucrose–hisitine solution, and excess DTT was removed by centrifugation. The pellet then was further washed twice with the same solution by centrifugation.

The resulting NBD-labeled enzyme preparations used in the present study contained 7.6 ± 1.2 nmol of NBD/mg of protein (average ± SD of 13 preparations). The modified amino acid residue was identified to be Cys-344 (Wakabayashi et al., 1990). The predominant effect of this NBD modification was inhibition of $Ca^{2+}$ release from the ADP-sensitive phosphoenzyme intermediate, which was responsible for the observed slow ATPase activity (5–10% of the control) (Wakabayashi et al., 1990).

The modified enzyme preparations were contaminated with 25–33 nmol of exchangeable calcium/mg of protein, as estimated by atomic absorption spectrometry of the EGTA-washed or nonwashed samples (Shigekawa et al., 1983). This exchangeable calcium was taken into account when the total $Ca^{2+}$ participating in the reaction was calculated.

*Fluorescence Measurements.* Equilibrium and transient kinetic fluorescence measurements were carried out at 11 °C in a standard medium containing 0.05–0.1 mg/mL of NBD-enzyme, 50 mM Mes/Tris (pH 6.5), 0.1 M KCl, and 2 mM $MgCl_2$ or otherwise under conditions described in the legend to each figure. Equilibrium fluorescence intensity of the NBD-enzyme was measured on a Hitachi MPF 4 spectrofluorometer as described previously (Wakabayashi et al., 1990). Rapid changes in the NBD fluorescence were monitored with a stopped-flow spectrofluorometer (Unisoku, FSS-300). For the latter measurements, excitation light, whose wavelength (430 nm) was selected with a monochromator, was further passed through a band-path filter (Corning 5-60) and emitted light was passed through a cutoff filter (Toshiba Y-49).

For the stopped-flow measurement of the NBD fluorescence rise induced by $Ca^{2+}$ ("on" fluorescence reaction), syringe A delivered the standard medium containing 0.2 mg/mL of NBD-enzyme and 0.3–0.4 mM EGTA, whereas syringe B delivered an equal volume of the standard medium containing various concentrations of $CaCl_2$ and other ligands. For the stopped-flow measurement of the NBD fluorescence decrease induced by $Ca^{2+}$ removal ("off" fluorescence reaction), syringe A delivered the standard medium containing 50–100 $\mu$M $CaCl_2$ and 0.2 mg/mL of NBD-enzyme, whereas syringe B delivered an equal volume of the standard medium containing various concentrations of EGTA. In some experiments (see Figure 2 and Results), quin 2 replaced EGTA to measure also the dissociation of the enzyme-bound calcium by monitoring

the quin 2 fluorescence change. In these experiments, 1 volume of the standard medium containing 1.5 mg/mL of enzyme and 50 $\mu$M $CaCl_2$ was mixed with 4 volumes of the standard medium containing 31–425 $\mu$M quin 2. When the effect of ADP on the quin 2-induced signals was examined (see Results), both the enzyme syringe and the quin 2 syringe contained 0.3 mM ADP additionally. Association of quin 2 with $Ca^{2+}$ was sufficiently fast because the quin 2 fluorescence change occurred instantaneously in the time scales used for these experiments (cf. Figure 2), when the reaction media containing no enzyme were mixed. For measurements of quin 2 fluorescence, the excitation wavelength selected was 340 nm and excitation light was passed through a 7-60 Corning band-path filter, while the emitted light was passed through a Y-49 Toshiba cutoff filter.

When records for the fluorescence transient are shown, each record represents data obtained after 5–30 accumulations. The amplitude of the fluorescence change is expressed as the percentage of the observed maximal change.

*Measurements of $Ca^{2+}$ Binding and Dissociation.* The time course of $Ca^{2+}$ binding to the enzyme was followed either spectrophotometrically by using a $Ca^{2+}$-sensitive dye, antipyrylazo III, or by measuring binding of $^{45}Ca^{2+}$ to the enzyme with a Bio-logic rapid filtration apparatus as described previously (Dupont, 1984; Wakabayashi et al., 1986). In the former type of experiments, the NBD-enzyme (2 mg/mL) was preincubated in the standard medium containing 0.4 mM EGTA and then mixed with an equal volume of the standard medium containing 100 $\mu$M antipyrylazo III and various concentrations of $CaCl_2$ by using an Aminco-Morrow stopped-flow apparatus. The changes in the absorption difference at 720 and 790 nm were monitored on an Aminco-SLM DW-2C dual-wavelength spectrophotometer. Unfortunately, very fast binding of $Ca^{2+}$ to the enzyme could not be followed by this method, because a transient artifactual absorption change occurred within an initial 0.2 s after the mixing of reaction media (cf. Figure 1B). In the rapid filtration experiments, [$^3$H]glucose was included in the reaction medium to determine the filter wet volume for calculation of unbound $^{45}Ca$ (Wakabayashi et al., 1986).

Rapid dissociation of the enzyme-bound calcium was followed fluorometrically with the use of quin 2 as described above.

*Simulation of Experimental Data.* Simulations were performed by numerical computations with the aid of a 32-bit work station (Apollo, DN4000) and a simulation language [advanced continuous simulation language (ACSL)] developed by Mitchell and Gauthier Associates, Inc., using a fourth-order Runge–Kutta algorithm.

*Others.* The ionized $Ca^{2+}$ concentration at pH 6.5 and 11 °C was calculated by using apparent association constants of $10^{5.8}$ and $10^{6.4}$ $M^{-1}$ for calcium–EGTA and calcium–quin 2 complexes, respectively. The above value of the apparent association constant for the calcium–EGTA complex was obtained as described previously (Shigekawa et al., 1983). The apparent association constant for the calcium–quin 2 complex was estimated by comparing the $Ca^{2+}$ concentration dependence of the equilibrium NBD fluorescence levels measured in the presence of various concentrations of quin 2 with that measured in the presence of various concentrations of EGTA. Determination of protein concentrations and preparations of Tris/ATP and Tris/ADP were carried out as described in the previous paper (Shigekawa et al., 1983). GTP (Boehringer Mannheim) was purified by column chromatography on DEAE-Sephadex A-25 (Johnson & Walseth, 1979). The amount of ATP contaminating ADP was 1%, whereas those contaminating AMPPNP and GTP were less than 0.1%. These ATP contaminations were estimated by the use of the luciferin–luciferase system (ATP bioluminescence LIS) purchased from Boehringer Mannheim. Antipyrylazo III was purchased from Nakarai Chemical Co. and quin-2 from Dojin Chemical Co. Hexokinase was purchased from Boehringer Mannheim. All other reagents were of analytical grade.

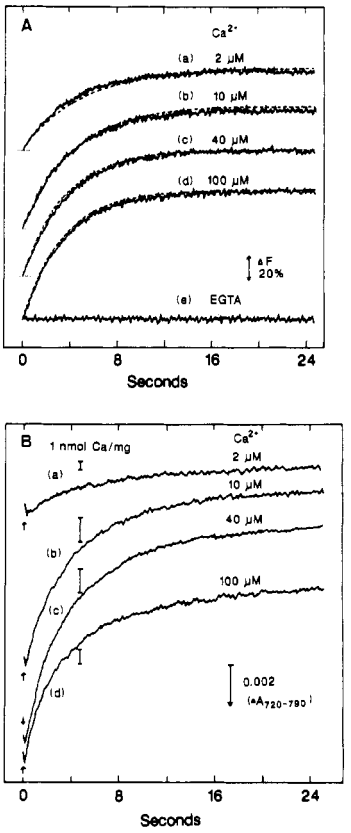


FIGURE 1: Records for (A) the rise in NBD fluorescence and (B) calcium binding following addition of $Ca^{2+}$ to the enzyme preincubated with EGTA. (A) The NBD-enzyme (0.2 mg/mL) preincubated in the standard medium containing 0.4 mM EGTA was mixed with an equal volume of the standard medium containing 0.22–0.59 mM $CaCl_2$ (traces a–d) or 0.4 mM EGTA (trace e). The time courses for fluorescence change were measured as described under Experimental Procedures. The broken line drawn through each trace is a simulated curve that was calculated by using the differential equations derived from Scheme III and values of parameters listed in Table I. (B) Time courses for $Ca^{2+}$ binding to the enzyme were followed spectrophotometrically by using antipyrylazo III as described under Experimental Procedures. Final ionized $Ca^{2+}$ concentrations are indicated in the figure. The height of the vertical bar given for each trace (a–d) represents the absorbance change that corresponds to binding of 1 nmol of $Ca^{2+}$/mg of protein. A scale for the absorbance change is also shown in the figure.

## RESULTS

*Kinetics of NBD Fluorescence Change, $Ca^{2+}$ Binding, and Dissociation.* Figure 1A shows typical traces for the fluorescence rise following addition of various concentrations of $CaCl_2$ to the NBD-enzyme preincubated with EGTA ($Ca^{2+}$-deprived enzyme). These $Ca^{2+}$-induced fluorescence transients were all monoexponential. Interestingly, the $k_{obs}$ value for the fluorescence rise changed minimally (from 0.25 to 0.27 $s^{-1}$) (Figure 1A; see also Figure 3) when $Ca^{2+}$ in the medium was varied from 2 to 100 $\mu$M. Figure 1B shows the time courses of $Ca^{2+}$ binding to the NBD-enzyme, which were measured optically by the use of antipyrylazo III under conditions similar to those for Figure 1A. Although these traces for the $Ca^{2+}$ binding could not be fitted completely to single

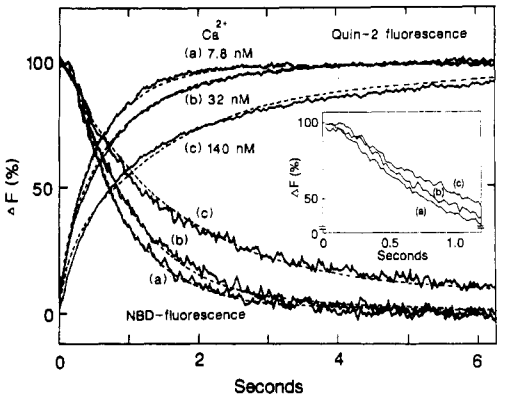


FIGURE 2: Records for calcium dissociation and decrease in NBD fluorescence induced by $Ca^{2+}$ removal. Time courses for both the $Ca^{2+}$ dissociation and the NBD fluorescence decrease following addition of quin-2 to the $Ca^{2+}$-saturated enzyme were measured under identical conditions (see Experimental Procedures). Final quin-2 concentrations were 340, 88, and 25 $\mu$M for traces a, b, and c, respectively, whereas the total $Ca^{2+}$ concentration was 10 $\mu$M. Thus, the corresponding ionized $Ca^{2+}$ concentrations present immediately after the addition of quin 2 would have been 7.8, 32, and 140 nM, respectively, since 10 nmol of $Ca^{2+}$ was initially bound by 1 mg of the ATPase protein (see inset to Figure 3). The broken line drawn through each trace is a simulated curve that was calculated by using the differential equations derived from Scheme III and values of parameters listed in Table I. The time-dependent increase in the ionized $Ca^{2+}$ concentration due to release of the enzyme-bound calcium caused by the quin 2 addition was taken into account when simulations of the data were performed. The inset shows traces for the NBD fluorescence decrease measured in a short time range.

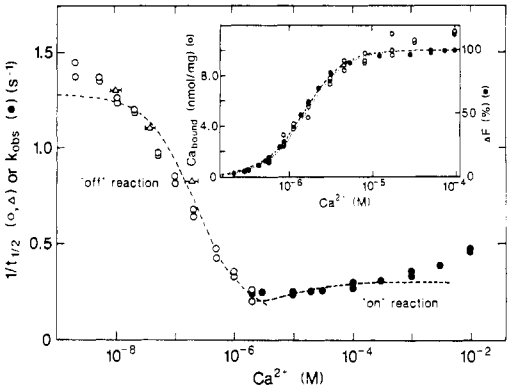


FIGURE 3: $Ca^{2+}$ concentration dependence of the rate constants for the on and off fluorescence reactions. The rate constants for the NBD fluorescence rise following addition of $Ca^{2+}$ to the $Ca^{2+}$-deprived enzyme (●) (cf. Figure 1A) and for the decrease in NBD fluorescence following addition of EGTA (○) or quin-2 (△) to the $Ca^{2+}$-bound enzyme (cf. Figure 2) were plotted as a function of the final concentration of ionized $Ca^{2+}$. The off rate constant was described as the reciprocal of the time at which half the maximal decrease in fluorescence occurred. The inset shows the $Ca^{2+}$ dependence of the equilibrium levels of $Ca^{2+}$ binding to the enzyme and NBD fluorescence, which were taken from our previous paper (Wakabayashi et al., 1990) to simply compare them with the simulated data. The broken and dotted lines show the simulated data that were calculated by using the differential equations derived from Scheme III and values of parameters listed in Table I. In the inset, the broken and dotted lines represent simulated curves for the equilibrium levels of NBD fluorescence and $Ca^{2+}$ binding, respectively.

exponentials, the approximate values of $k_{obs}$, which were estimated by fitting the initial 90–95% of these progress curves to single exponentials, were 0.22, 0.24, 0.24 and 0.27 $s^{-1}$ at 2, 10, 10, 40, and 100 $\mu$M $Ca^{2+}$, respectively. These results indicate that $Ca^{2+}$ binding proceeds at rates comparable to those for the on fluorescence change.

Figure 2 shows records for the NBD fluorescence change, which was induced by mixing the NBD-enzyme preincubated with a saturating concentration of $Ca^{2+}$ with various concentrations of quin 2, a fluorescent $Ca^{2+}$ chelator. The quin 2 induced decrease in NBD fluorescence, which could not be fitted to a single exponential except at the lowest $Ca^{2+}$ concentration used (7.8 nM), was preceded by an obvious initial lag of 0.1–0.2 s (see inset). Figure 2 also shows records for the increase in quin 2 fluorescence measured under exactly the same experimental conditions to follow the release of $Ca^{2+}$ from the enzyme. The quin 2 signal neither exhibited an initial lag nor followed a simple exponential time course. In addition, it proceeded at a faster rate than the corresponding NBD signal; in the presence of 7.8 and 140 nM ionized $Ca^{2+}$, the half-times for the quin 2 signal were 0.34 and 0.72 s, whereas those for the NBD signal were 0.72 and 1.2 s, respectively. Thus, $Ca^{2+}$ release from the enzyme was faster than the off NBD fluorescence change. It should be noted that these two processes became markedly slower when the ionized $Ca^{2+}$ concentration in the reaction medium increased (Figure 2; see also Figure 3).

Figure 3 shows the dependences on the ionized $Ca^{2+}$ concentration of the $k_{obs}$ values for the on NBD fluorescence change and of the reciprocal of the half-times for the off NBD fluorescence change. The reciprocal of the half-time for the off reaction decreased sharply with increasing $Ca^{2+}$ concentrations, reaching the minimum at ~1–2 $\mu$M $Ca^{2+}$. Half-maximal decrease occurred at ~0.1–0.2 $\mu$M $Ca^{2+}$. On the other hand, the rate constant for the on reaction increased only slightly when the $Ca^{2+}$ concentration was raised from 1 to 200 $\mu$M, although it clearly increased further at millimolar $Ca^{2+}$ concentrations (Figure 3). For a comparative purpose, the inset shows the $Ca^{2+}$ concentration dependence of $Ca^{2+}$ binding to the enzyme and the accompanying NBD fluorescence change measured under equilibrium conditions (Wakabayashi et al., 1990).

*Effect of Nucleotides on Kinetics of NBD Fluorescence Change.* In our previous paper (Wakabayashi et al., 1990), we showed that added ATP raised the equilibrium level of NBD fluorescence in the $Ca^{2+}$-deprived enzyme and that the ATP concentration dependence of this fluorescence change was almost identical with that for the equilibrium binding of ATP to the enzyme measured under the same conditions. Since the observed maximum level of ATP binding (~5–6 nmol/mg) almost corresponded to the maximum level of phosphoenzyme formed, we concluded that the NBD fluorescence change was induced by binding of 1 mol of ATP/mol of the enzyme active center. In the presence of EGTA at pH 6.5 and 11 °C, the conditions used in this study, about 30 $\mu$M ATP produced half-maximal effects on the NBD fluorescence level and the ATP binding. Under these conditions, the maximum level of the NBD fluorescence rise induced by saturating concentrations of ATP was about 70% that of the $Ca^{2+}$-induced change.

Figure 4 shows the time course of the NBD fluorescence rise following addition of ATP (final concentration 300 $\mu$M) to the $Ca^{2+}$-deprived enzyme. The fluorescence rise consisted of fast and slow phases, both of which proceeded monoexponentially. We considered the slow component to be derived from the fast component in a side reaction and not to be directly involved in $Ca^{2+}$ binding and release (see Discussion).

In the experiment shown in Figure 5, the time courses of the NBD fluorescence rise were followed after addition of mixtures of ATP (final concentration 0.3 mM) and various concentrations of $Ca^{2+}$ to the $Ca^{2+}$-deprived enzyme. At low ionized $Ca^{2+}$ concentrations (~1–2 $\mu$M), the fluorescence rise was not monophasic. The initial fast phase probably arose

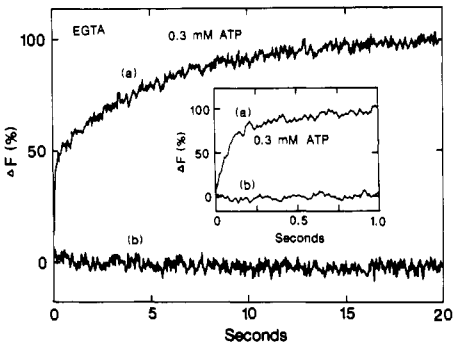


FIGURE 4: Records for the ATP-induced NBD fluorescence increase in the $Ca^{2+}$-deprived enzyme. The NBD-enzyme (0.2 mg/mL) in the standard medium containing 0.3 mM EGTA was mixed with an equal volume of the standard medium containing either 0.6 mM ATP and 0.3 mM EGTA (trace a) or 0.3 mM EGTA (trace b), and time courses for fluorescence change were followed as described under Experimental Procedures. The inset shows traces for the fluorescence change measured in a short time range.

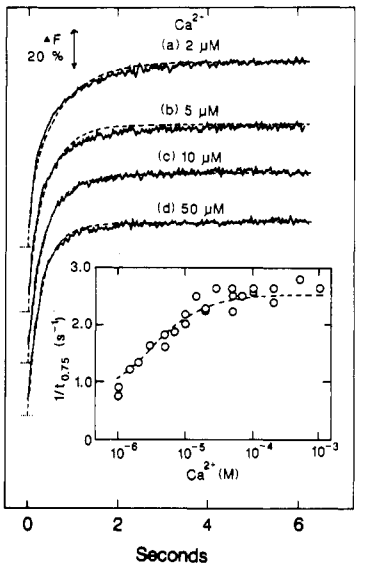


FIGURE 5: Effect of $Ca^{2+}$ concentrations on the time course for the ATP-induced fluorescence rise. The NBD-enzyme (0.2 mg/mL) in the standard medium containing 0.3 mM EGTA was mixed with an equal volume of the standard medium containing 0.6 mM ATP (final concentration 0.3 mM) and 0.106–2.3 mM $CaCl_2$, and time courses for the fluorescence rise were followed as described under Experimental Procedures. The final concentrations of ionized $Ca^{2+}$ are indicated in the figure. The inset plots the reciprocal of the time required for 75% completion of the fluorescence rise as a function of the $Ca^{2+}$ concentration. The broken lines drawn through each trace in the figure and through the data points in the inset are the simulated curves that were calculated by using the differential equations derived from Scheme III and values of parameters listed in Table I. For these simulations, the apparent forward ($k_1$) and reverse ($k_{-1}$) rate constants for step 1 of Scheme III in the presence of 0.3 mM ATP were calculated by using eqs 1 and 2 of the Appendix and values of parameters listed in Table I (for $k''_1$, a value of 4.1 $s^{-1}$ was used).

from ATP binding to the $Ca^{2+}$-deprived enzyme (cf. Figure 4). The late, slow phase could be a mixture of the $Ca^{2+}$-induced fluorescence increase, which would be slow due to the low $Ca^{2+}$ concentrations used, and the very slow component of the ATP-induced fluorescence rise observed in the $Ca^{2+}$-deprived enzyme (cf. Figure 4). The late, slow phase of the fluorescence rise was accelerated as the concentration of $Ca^{2+}$ increased and the entire time course of the fluorescence rise became monoexponential at $Ca^{2+}$ concentrations higher than 40 μM.

In the inset to Figure 5, we plotted the reciprocal of the time required for 75% completion of the fluorescence rise as a function of the ionized $Ca^{2+}$ concentration. The remarkable $Ca^{2+}$ concentration dependence observed in the presence of ATP (Figure 5, inset) was in sharp contrast to the lack of $Ca^{2+}$ dependence found in the absence of ATP (Figure 3). The apparent $Ca^{2+}$ concentration at which half-maximal effect was observed was less than 10 μM under the conditions of Figure 5.

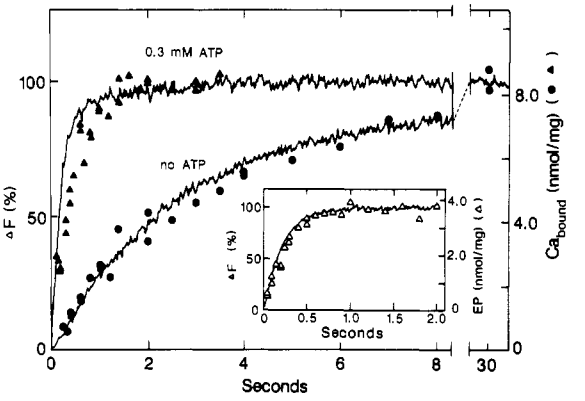


FIGURE 6: Effects of ATP on time courses for $Ca^{2+}$ binding and the rise in NBD fluorescence. The time courses of $^{45}Ca^{2+}$ binding to the enzyme were measured by using a rapid filtration apparatus by washing the EGTA-pretreated enzyme immobilized on the membrane filter with a solution containing 50 mM Mes/Tris (pH 6.5), 0.1 M KCl, 2 mM $MgCl_2$, 50 μM $^{45}CaCl_2$, 10 mM $^3$H-glucose, and either 0 (●) or 0.3 mM ATP (▲). For the measurement of fluorescence rise, the NBD-enzyme (0.2 mg/mL) preincubated in 0.3 mM EGTA was mixed with an equal volume of the standard medium containing 0.4 mM $CaCl_2$ and 0 or 0.6 mM ATP. The inset shows time courses for the rise in NBD fluorescence and the formation of phosphoenzyme. The latter was measured by using a simple mixing apparatus as described previously (Shigekawa & Kanazawa, 1982) by adding 0.04 mL of a mixture of [γ-$^{32}$P]ATP and $CaCl_2$ to 0.96 mL of a medium containing 0.3 mg/mL of the NBD-enzyme and 0.3 mM EGTA. The final concentrations of ATP, $Ca^{2+}$, and other salts in the phosphorylation medium were the same as those used for the fluorescence measurement.

Figure 6 shows the effect of the presence or absence of 0.3 mM ATP on the $Ca^{2+}$-induced NBD fluorescence rise and $^{45}Ca^{2+}$ binding. $^{45}Ca$ binding was measured by using a rapid membrane filtration apparatus (see Experimental Procedures). In the absence of ATP, the fluorescence rise proceeded at a rate similar to that for the $^{45}Ca^{2+}$ binding, as already shown in Figure 1. In the presence of ATP, both the $Ca^{2+}$-induced fluorescence transient and $^{45}Ca^{2+}$ binding were accelerated by a factor of about 10. The inset to Figure 6 shows progress curves for the rise in NBD fluorescence and the formation of phosphoenzyme measured with the same enzyme preparation under comparable conditions. These latter processes proceeded monoexponentially at similar rates of 4.3 and 3.5 $s^{-1}$, respectively, without showing initial induction periods. Comparison of the time courses of phosphoenzyme formation (Figure 6 inset, △) and $^{45}Ca^{2+}$ binding (Figure 6, ▲) revealed that the former was slightly faster than the latter. Since the latter presumably precedes the former, it is likely that the membrane filtration method was not able to follow very fast $^{45}Ca^{2+}$ binding accurately.

In Figure 7A, we show the ATP concentration dependence of the $k_{obs}$ value for the monoexponential NBD fluorescence rise measured after the $Ca^{2+}$-deprived enzyme was mixed with $CaCl_2$ (final concentration 0.5 mM) plus various concentrations of ATP. The on fluorescence rate constant increased with an increasing ATP concentration, reaching a plateau value of 3–4 $s^{-1}$ at 200 μM ATP. A half-maximal stimulation was observed at 60–70 μM ATP. Essentially the same ATP concentration dependence was obtained when a lower con-

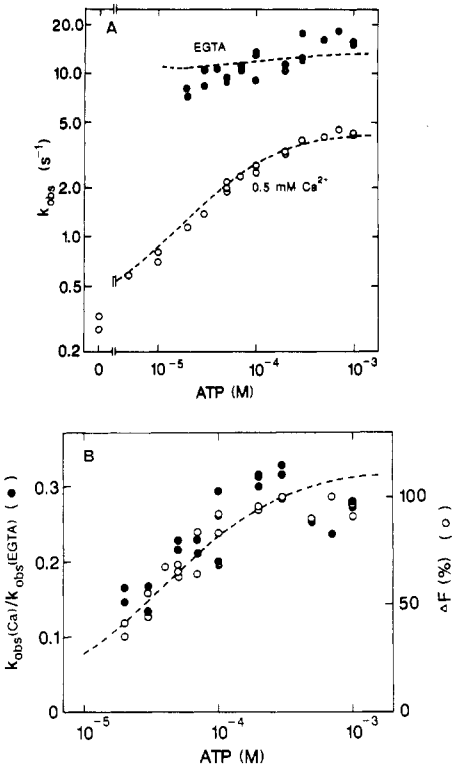


FIGURE 7: ATP dependence of (A) the $k_{obs}$ values for the rise in NBD fluorescence in the presence or absence of $Ca^{2+}$ and of (B) the ratio between these $k_{obs}$ values. (A) The NBD-enzyme (0.2 mg/mL) in the standard medium containing 0.3 mM EGTA was mixed with an equal volume of the standard medium containing various concentrations of ATP and either 1.3 mM $CaCl_2$ (final $Ca^{2+}$ concentration 0.5 mM) (○) or 0.3 mM EGTA (●). The $k_{obs}$ values for the $Ca^{2+}$-induced fluorescence rise (○) and for the initial fast phase of the ATP-induced fluorescence rise in the $Ca^{2+}$-deprived enzyme (●) (cf. Figure 4) were plotted against the ATP concentration. (B) The ratio (●) between the above $k_{obs}$ values was plotted against the ATP concentration. In (B), the amplitude of the initial fast phase of the ATP-induced fluorescence rise measured in the $Ca^{2+}$-deprived enzyme (cf. Figure 4) was also plotted (○). The broken lines in (A) were drawn according to eqs 1–3 of the Appendix by using values of parameters listed in Table I (for $k''_1$, a value of 4.3 $s^{-1}$ was used). In (B), the broken line shows the ATP dependence of the ratio $k_1/(k_{-1} + k_1)$, which was calculated by using the same set of values of the parameters as that used for (A).

centration of $Ca^{2+}$ (40 μM) was used in otherwise the same type of experiment (cf. Figure 8A). In Figure 7A, we also show the ATP dependence of the $k_{obs}$ value for the initial fast phase of the ATP-induced fluorescence rise measured in the $Ca^{2+}$-deprived enzyme (in the presence of excess EGTA) (cf. inset to Figure 4). The $k_{obs}$ value was ~7–10 $s^{-1}$ at ~20–30 μM ATP, which increased slightly at higher ATP concentrations (>300 μM).

We calculated the ratio between the $k_{obs}$ value measured in the presence of $Ca^{2+}$ [Figure 7A (○)] and the corresponding value measured in the presence of excess EGTA [Figure 7A (●)] and plotted it against the ATP concentration [Figure 7B (●)]. We also plotted the amplitude of the fast component of the ATP-induced fluorescence rise measured in the $Ca^{2+}$-deprived enzyme (cf. Figure 4) as a function of ATP concentration [Figure 7B (○)]. As shown in Figure 7B, the ATP dependence of both processes is similar. It is also similar to that for the equilibrium fluorescence rise (cf. Figure 8B) and for the equilibrium ATP binding [cf. Wakabayashi et al. (1990)]. It should be pointed out here that the effective range of ATP concentration (~30–40 μM) measured in these experiments is significantly lower than that (~60–70 μM) obtained from the ATP dependence of the on fluorescence rate

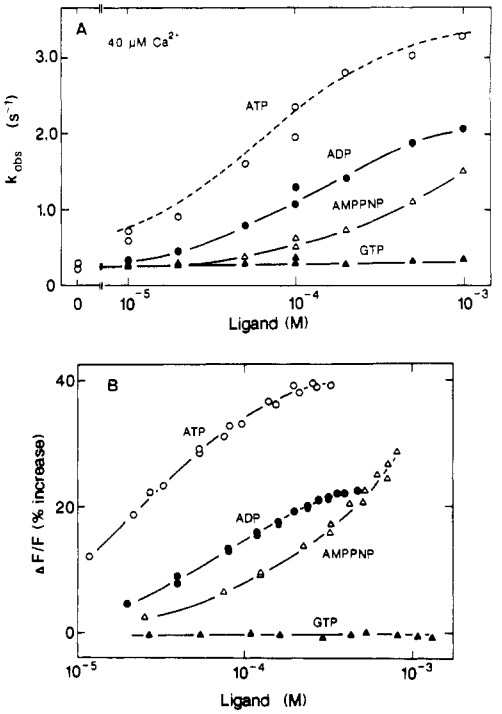


FIGURE 8: Effects of nucleotides on (A) the $k_{obs}$ value for the $Ca^{2+}$-induced NBD fluorescence rise and on (B) the equilibrium level of NBD fluorescence in the $Ca^{2+}$-deprived enzyme. (A) The NBD-enzyme (0.2 mg/mL) in the standard medium containing 0.4 mM EGTA was mixed with an equal volume of the standard medium containing 0.48 mM $CaCl_2$ (final $Ca^{2+}$ concentration 40 μM) and various concentrations of nucleotides. The $k_{obs}$ values calculated from the monoexponential time courses for the NBD fluorescence rise (cf. Figure 6) were plotted against the concentration of each nucleotide used. The broken line for the ATP data was drawn according to eq 1 of the Appendix by using values of parameters listed in Table I (for $k''_1$, a value of 3.5 $s^{-1}$ was used). (B) Equilibrium levels of NBD fluorescence were measured with 0.1 mg/mL of the enzyme in the standard medium containing 0.3 mM EGTA and the indicated concentrations of various nucleotides.

constant (Figures 7A and 8A). This difference will be discussed later (see Discussion).

In Figure 8A, we examined the effect of various ATP analogues on the $k_{obs}$ value for the monoexponential NBD fluorescence rise in the presence of 40 μM $Ca^{2+}$. ATP was most effective among the nucleotides tested; the extent of its maximal activation (12-fold) and its concentration (60 μM) to give a half-maximal effect were similar to those obtained in the experiment described above [Figure 7A (○)]. The corresponding values for these parameters for ADP were 7.8-fold and ~100 μM, respectively. In the case of AMPPNP, the $k_{obs}$ value increased with increasing concentrations of this nucleotide without showing a sign of saturation even at 1 mM, indicating that the enzyme affinity for this nucleotide was significantly less than that for ATP or ADP. Because the result was similar when ADP or AMPPNP was treated with hexokinase and glucose, the contaminating ATP was not responsible for the observed effects of these ATP analogues. GTP was ineffective even at 1 mM.

In Figure 8B, for a comparative purpose, we show the nucleotide concentration dependence of the equilibrium NBD fluorescence level measured in the absence of $Ca^{2+}$. In accordance with the data shown in Figure 8A, ATP, ADP, and AMPPNP markedly increased the equilibrium level of NBD fluorescence, whereas GTP was ineffective.

Figure 9 shows the result of an experiment in which the equilibrium binding of [$^{14}$C]ADP to the NBD-enzyme was measured in the presence or absence of $Ca^{2+}$. Scatchard

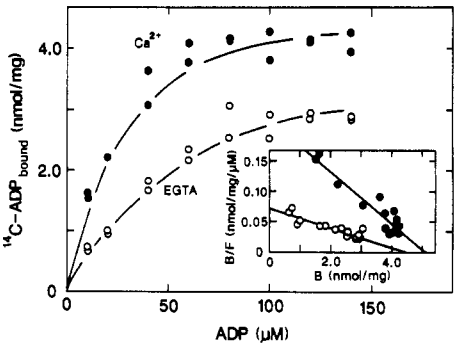


FIGURE 9: Equilibrium ADP binding to the enzyme in the presence or absence of $Ca^{2+}$. The amount of [$^{14}$C]ADP bound to the enzyme was measured with 0.1 mg/mL of NBD-enzyme in the standard medium containing 10 mM [$^3$H]glucose, various concentrations of [$^{14}$C]ADP, and either 0.1 mM $CaCl_2$ (●) or 0.3 mM EGTA (○) by the membrane filtration method (Shigekawa et al., 1983). The inset shows Scatchard plots of the data.

analysis of the data shows that the maximal amount of ADP bound ($B_{max}$) and the dissociation constant ($K_d$) for ADP are 5.1 nmol/mg of protein and 23 μM in the presence of 0.1 M $Ca^{2+}$ and 4.5 nmol/mg of protein and 63 μM in the presence of 0.3 mM EGTA. As in the case of ATP (see above), the apparent affinities for ADP estimated from this experiment were significantly higher than that estimated from the transient kinetic measurement in Figure 8A.

Finally, we examined whether ADP, an ATP analogue that accelerated the on fluorescence reaction (see above), also activates the off reaction (cf. Figure 2). We measured the effect of 0.3 mM ADP on the time courses for the decrease of the NBD fluorescence and the increase in the quin 2 fluorescence, both of which were induced by adding quin 2 to the $Ca^{2+}$-saturated enzyme preincubated with or without ADP (see Experimental Procedures for details). In this experiment, the final concentrations of quin 2 and ionized $Ca^{2+}$ after the quin 2 addition were 340 μM and 8 nM, respectively. The $Ca^{2+}$ release, which was monitored by the quin 2 fluorescence increase, was not accelerated greatly by ADP; the half-times were 0.36 and 0.44 s with and without 0.3 mM ADP, respectively. The half-times for the NBD fluorescence decrease also changed slightly, from 0.74 s without ADP to 0.62 s with 0.3 mM ADP.

## Discussion

*Mechanism of Activation of $Ca^{2+}$-ATPase by $Ca^{2+}$.* Our experiments in the absence of ATP revealed the following features of $Ca^{2+}$-induced activation of the NBD-enzyme under the standard conditions of this study (pH 6.5, 2 mM $MgCl_2$, and 11 °C): (a) The NBD fluorescence rise upon addition of $Ca^{2+}$ (1–100 μM) was monoexponential, and its $k_{obs}$ value was almost independent of the added $Ca^{2+}$ concentration (Figures 1A and 3). (b) The rates of $Ca^{2+}$ binding to the NBD-enzyme at $Ca^{2+}$ concentrations from 2 to 100 μM were slow and almost equal to those for the NBD fluorescence rise measured under the same conditions (Figures 1 and 6). (c) Neither the NBD fluorescence decrease nor the $Ca^{2+}$ dissociation following reduction of the free $Ca^{2+}$ concentration in the medium proceeded monoexponentially except when the final $Ca^{2+}$ concentration was very low (<~10 nM). Under the latter conditions, the NBD fluorescence decrease, but not the $Ca^{2+}$ dissociation, was preceded by an initial induction period (Figure 2). (d) $Ca^{2+}$ dissociation from the enzyme proceeded at a significantly faster rate than the NBD fluorescence decrease (Figure 2). The apparent rates of both processes decreased markedly with increasing $Ca^{2+}$ concentrations in the medium (Figures 2 and 3).

In addition to (a) described above, we found that the $Ca^{2+}$-induced NBD fluorescence rise was monoexponential at pH 7.2 and 5 mM $MgCl_2$.[2] These findings are in sharp contrast to the observations by others that both the intrinsic protein fluorescence (Champeil et al., 1983) and EDANS fluorescence (Suzuki et al., 1987) produce biphasic on signals at neutral pH in the presence of millimolar $Mg^{2+}$. Thus, different probes may monitor different conformational changes involved in the enzyme activation by $Ca^{2+}$.

Points (c) and (d) above demonstrate that the kinetics of $Ca^{2+}$ dissociation and the NBD fluorescence decrease are clearly different. This indicates that the NBD fluorescence change does not simply monitor the conformational change associated with the local occupancy of the $Ca^{2+}$-binding sites (see the introduction). As the NBD fluorescence changes associated with isomerizations in the unphosphorylated and phosphorylated enzymes at pH 6 were shown to be of the same size but in the opposite direction (Wakabayashi et al., 1990), it seems likely that the NBD signal monitors the conformational transition like the one postulated for the putative $E_1$–$E_2$ model (de Meis & Vianna, 1979) (see the introduction).

As stated in the introduction, the two calcium sites on the enzyme are not kinetically identical, and dissociation of the enzyme-bound calcium follows an ordered process (Ikemoto et al., 1981; Dupont, 1982; Inesi, 1987; Petithory & Jencks, 1988a). Sequential binding and dissociation of $Ca^{2+}$ involving a major enzyme isomerization step could occur in one of the following three simple schemes (Schemes I–III), some of which have already been described (Champeil et al., 1983; Fernandez et al., 1984; Froud & Lee, 1986; Petithory & Jencks, 1988b).

Scheme I

$$E_2 \overset{Ca^{2+}}{\rightleftharpoons} E_2Ca \overset{Ca^{2+}}{\rightleftharpoons} E_2Ca_2 \rightleftharpoons E_1Ca_2$$

Scheme II

$$E_2 \underset{k_{-1}}{\overset{k_1[Ca^{2+}]}{\rightleftharpoons}} E_2Ca \underset{k_{-2}}{\overset{k_2}{\rightleftharpoons}} E_1Ca \underset{k_{-3}}{\overset{k_3[Ca^{2+}]}{\rightleftharpoons}} E_1Ca_2$$

Scheme III

$$E_2 \underset{k_{-1}}{\overset{k_1}{\rightleftharpoons}} E_1 \underset{k_{-2}}{\overset{k_2[Ca^{2+}]}{\rightleftharpoons}} E_1Ca \underset{k_{-3}}{\overset{k_3[Ca^{2+}]}{\rightleftharpoons}} E_1Ca_2$$

In these schemes, we designate two different enzyme conformations as $E_1$ and $E_2$ and assume that the NBD fluorescence rises when $E_2$ is converted into $E_1$. Scheme I cannot account for some of the observations in (a), (c), and (d) described above. On the other hand, the model in Scheme II can simulate the kinetics of the NBD fluorescence change fairly well, assuming $k_{-1}/k_1 = 2 \times 10^{-6}$ M, $k_{-1} > 10$ s$^{-1}$, $k_2 = 0.3$ s$^{-1}$, $k_{-2} = 1.3$ s$^{-1}$, $k_3 = 3.5 \times 10^7$ M$^{-1}$ s$^{-1}$, and $k_{-3} = 6$ s$^{-1}$. Unique values for these rate constants except for $k_1$ and $k_{-1}$ were determined from the value of the on rate constant in relatively high $Ca^{2+}$ (Figure 3) and from simulations of kinetics of both the off NBD fluorescence change and $Ca^{2+}$ dissociation in the presence of various ionized $Ca^{2+}$ concentrations (Figure 2). The value of $k_1/k_{-1}$ was determined from simulation of the equilibrium NBD fluorescence data (Figure 3, inset). These values of the rate constants predict rapid accumulation of $E_2Ca$ at 2–100 μM $Ca^{2+}$. However, this was not experimentally observed as described in the above (b).

Unlike Schemes I and II, Scheme III can explain all of the present data. Again, unique values for the rate constants could

[2] S. Wakabayashi and M. Shigekawa, unpublished observation.

Table I: Parameters Describing ATPase Activation by $Ca^{2+}$ and ATP[a]

| parameters | values | parameters | values |
|---|---|---|---|
| $k_1$, $k'_1$ | 0.3 $s^{-1}$ | $k_{-2}$ | 1.6 $s^{-1}$ |
| $k''_1$ | ~3.5–4.3 $s^{-1}$ | $k_3$ | $3.5 \times 10^7$ $M^{-1}$ $s^{-1}$ |
| $k_{-1}$, $k'_{-1}$ | 20 $s^{-1}$ | $k_{-3}$ | 5 $s^{-1}$ |
| $k''_{-1}$ | 9 $s^{-1}$ | $K_1$ | 1.9 ~ 2.3 $\mu$M |
| $k_2$ | $8 \times 10^6$ $M^{-1}$ $s^{-1}$ [b] | $K_2$ | 60 $\mu$M |
| | $4 \times 10^6$ $M^{-1}$ $s^{-1}$ [c] | $K_a$ | 1 |

[a] Parameters are defined in Schemes III and IV. Values for these parameters were obtained by simulations of the experimental data with the models shown in Schemes III and IV (see the text). $k'_1$ and $k'_{-1}$ or $k''_1$ and $k''_{-1}$ in Scheme IV, which are the rate constants for the non-ATP-bound or ATP-bound enzyme, respectively, can be correlated with $k_1$ and $k_{-1}$ of Scheme III according to eqs 1 and 2 of the Appendix. [b] Estimated from the data in the absence of ATP. [c] Estimated from the data in 0.3 mM ATP (see Figure 5).

be determined either experimentally ($k_2$) or from simulations of the data shown in Figures 1A, 2, and 3 ($k_1$, $k_{-1}$, $k_{-2}$, $k_3$, and $k_{-3}$) (see Table I). The broken and dotted lines in these figures show that we successfully reproduce both the equilibrium and transient kinetic data in the absence of ATP. We conclude therefore that Scheme III is appropriate to describe the mechanism of enzyme activation by $Ca^{2+}$ under the conditions of our experiments. According to Table I, both the first and second $Ca^{2+}$ ions bind to the enzyme with high affinity ($K_d$ ~0.1–0.4 $\mu$M) and the equilibrium between $E_1$ and $E_2$ in the absence of $Ca^{2+}$ is shifted mostly to $E_2$. At relatively low $Ca^{2+}$ concentrations (<100 $\mu$M), therefore, $Ca^{2+}$ binding occurs only after the major conformational transition of the enzyme from the $E_2$ state, which cannot bind $Ca^{2+}$ with high affinity, to the $E_1$ state having high affinity for $Ca^{2+}$. This conclusion is in accord with the original $E_1$–$E_2$ concept (de Meis & Vianna, 1979).

According to Table I, the $E_2$ to $E_1$ conversion is the slowest step in the overall forward reaction under the conditions used in this study. Petithory and Jencks (1988b) have recently studied the kinetics of $Ca^{2+}$ binding by the enzyme under the conditions (pH 7.0, 25 °C, and 5 mM $Mg^{2+}$) that were significantly different from those used here. They rejected the reaction model in which a slow conformational change precedes rapid binding and dissociation of $Ca^{2+}$. Our model is not incompatible with their conclusion, because in our model the rate-limiting step in the overall reverse reaction is not the conformational change but the dissociation of $Ca^{2+}$ from the enzyme (Table I).

Another comment on our simulation with Scheme III is that the model may be too simple to describe the kinetics of enzyme activation by high $Ca^{2+}$. The values of the rate constant for the $Ca^{2+}$-induced NBD fluorescence rise deviated significantly from the calculated ones when the $Ca^{2+}$ concentration exceeded about 3 mM (Figure 3). It thus appears that $Ca^{2+}$ also binds to the low-affinity site, which could bring about faster conformational transition. Such a low-affinity pathway has recently been postulated by Petithory and Jencks (1988b), although the optimal $Ca^{2+}$ concentration for the low-affinity site detected in their study appears to be much lower than millimolar concentrations. The latter difference may be due to the difference in the experimental conditions used.

*Mechanism of the ATP-Induced Acceleration of $Ca^{2+}$ Binding to $Ca^{2+}$-ATPase.* It has been well documented that ATP accelerates enzyme activation by $Ca^{2+}$ (de Meis & Vianna, 1979; Inesi et al., 1980; Scofano et al., 1979). We confirmed this phenomenon by showing that the rate of $Ca^{2+}$ binding to the unphosphorylated enzyme increased markedly in the presence of ATP (Figure 6). We also showed that the monoexponential NBD fluorescence rise induced by the addition of $Ca^{2+}$ (final concentrations 40, 50, and 500 $\mu$M) was accelerated up to more than 10-fold by ATP or some other nucleotides (Figures 6–8).

Scheme IV

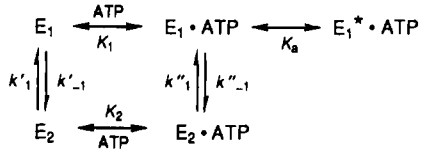


ATP addition in the absence of $Ca^{2+}$ induced the NBD fluorescence rise, which consisted of monoexponential fast and slow components (Figure 4). Because formation of the slow component was extremely slow, we consider it not to be involved directly in $Ca^{2+}$ binding. The intriguing question is whether the ATP-induced fast component represents an obligatory intermediate involved in $Ca^{2+}$ binding in the presence of ATP. The present finding (Figure 7B) that the amplitude of this ATP-induced fast fluorescence rise exhibited almost the same ATP concentration dependence as the ratio between the $k_{obs}$ value for the ATP-induced fluorescence rise in the presence of $Ca^{2+}$ (Figure 7A, ○) and the corresponding $k_{obs}$ value in the absence of $Ca^{2+}$ (Figure 7A, ●) strongly suggests that the ATP-induced fast component represents the high-fluorescence state, $E_1$, if Scheme III can be used to describe the kinetics of the NBD fluorescence change in the presence of ATP. This is because, in Scheme III, the value for the above ratio would give the amount of $E_1$ formed after the ATP-induced, rapid equilibration between $E_2$ and $E_1$, as the $k_{obs}$ obtained in the presence of a saturating $Ca^{2+}$ would correspond to the forward rate constant ($k_1$) for the $E_2$ to $E_1$ transition, whereas the $K_{obs}$ in the absence of $Ca^{2+}$ would correspond to a sum of the forward ($k_1$) and reverse ($k_{-1}$) rate constants.

In this study, interaction of the nucleotide with the enzyme was evaluated by analyzing the nucleotide concentration dependence of various ATP-dependent reactions. Interestingly, the effective nucleotide concentrations for these reactions were similar but not the same (Figures 7 and 8; Results). These differences can be accounted for by the following model (Scheme IV), which is a modification of the model in Scheme III. $K_1$ and $K_2$ are the ATP dissociation constants of $E_1$·ATP and $E_2$·ATP complexes, respectively. ATP binding to the enzyme is assumed to be fast as compared to the rate of the conformational transition. $E_1$*·ATP is an enzyme state with an elevated NBD fluorescence whose existence was detected in the $Ca^{2+}$-deprived enzyme as the ATP-induced slow component (Figure 4) (see above). $K_a$, which is an equilibrium constant for the $E_1$·ATP ↔ $E_1$*·ATP transitions, was estimated to be about 1 (Figure 4). $k'_1$ and $k'_{-1}$ are the forward and reverse rate constants for the $E_2$ to $E_1$ transition in the non-ATP-bound enzyme, whereas $k''_1$ and $k''_{-1}$ are the corresponding rate constants in the ATP-bound enzyme. These kinetic parameters can be correlated with $k_1$ and $k_{-1}$ of Scheme III according to eqs 1 and 2 of the Appendix.

Schemes III and IV can successfully simulate the complex kinetics of the NBD fluorescence changes in the presence of ATP (see broken lines in Figures 5, 7, and 8A) by using the values for the kinetic parameters listed in Table I. The values for $k''_1$, $k''_{-1}$, $K_1$, and $K_2$ were estimated from simulations of the ATP dependence of the $k_{obs}$ values for the NBD fluorescence rise in the presence and absence of $Ca^{2+}$ (Figures 7A and 8A; see also eqs 1–3 of the Appendix). These latter values satisfy a thermodynamic relationship, $K_2 k''_{-1}/k''_1 = K_1 k'_{-1}/k'_1$.

For simulations, we assume that ATP does not affect the rate constants for binding and release of $Ca^{2+}$ except for $k_2$ (Table I). These values of the parameters are compatible with the time course of phosphorylation of the $Ca^{2+}$-deprived enzyme by ATP plus $Ca^{2+}$ (Figure 6), which did not exhibit a significant initial induction period.

Two interesting points become apparent from these analyses. One is that ATP binds to $E_2$ with intermediate affinity of $K_2$ = 60 $\mu$M and to $E_1$ with high affinity of $K_1 = \sim 2$ $\mu$M (Table I). Because $k''_1 \gg k'_1$, the estimated $K_2$ value (60 $\mu$M) gives the $ATP_{1/2}$ value for the on fluorescence reaction (Figures 7A and 8A). We calculate $ATP_{1/2}$ values of 41–44 $\mu$M for the amplitude of the fast component of the ATP-induced fluorescence rise in the $Ca^{2+}$-deprived enzyme (Figure 7B) and 31–34 $\mu$M for the equilibrium NBD fluorescence level in the $Ca^{2+}$-deprived enzyme (Figure 8B) by using eqs 4 and 5 of the Appendix and the values of kinetic parameters listed in Table I. These $ATP_{1/2}$ values agree with the experimentally determined values. Thus, the model in Scheme IV can readily explain the differences in the $ATP_{1/2}$ values for the various ATP-dependent reactions.

Another interesting point is that in Scheme IV the enzyme is assumed to have only a single site for ATP. Involvement of a single ATP-binding site in acceleration of $Ca^{2+}$ binding is supported by our previous observations (Wakabayashi et al., 1990) that both the ATP binding and the NBD fluorescence rise at equilibrium exhibited identical ATP concentration dependence in the absence of $Ca^{2+}$ and that, under the same experimental setting, 1 mol of ATP/mol of the phosphorylation site was maximally bound by the enzyme. The data of Figure 9, in addition, show that ADP, which, like ATP, accelerated the $E_2$ to $E_1$ transition (Figure 8A), was also bound by the enzyme at a molar ratio of 1/1 both in the presence and absence of $Ca^{2+}$. These findings are consistent with the previous result (Stahl & Jencks, 1984) that, at pH 7 and 25 °C, ATP bound at a single site with high affinity ($K_d$ 4–5 $\mu$M) is responsible for acceleration of the conformational change associated with $Ca^{2+}$ binding.

Unlike ATP, GTP even at 1 mM did not accelerate the enzyme isomerization (Figure 8A). Adenine-containing ATP analogues such as ADP and AMPPNP increased the value of $k_1$ in Scheme III, although to a significantly less extent than ATP. These data, which are consistent with the previous reports (de Meis & Masuda, 1974; de Meis & Boyer, 1978) that GTP and ITP are much less effective than ATP in inhibiting phosphorylation of the enzyme by $P_i$, suggest that the base moiety of the nucleotide is important in determining the affinity of the enzyme for the nucleotides. As discussed above, the $E_1$ state of the enzyme exhibited a significantly higher affinity for ATP relative to the $E_2$ state (Table I). This was also true with ADP (Figures 8 and 9; see also Results). This appears to be true also with GTP, because the enzyme can be phosphorylated by micromolar GTP in the presence of $Ca^{2+}$ (de Meis et al., 1973).

Finally, we point out that the off reactions (release of the enzyme-bound calcium and NBD fluorescence decrease) were affected minimally by ADP at a concentration which accelerated the $E_2$ to $E_1$ transition (see Results). This finding is consistent with a previous report (Petithory & Jencks, 1988a), which showed that the dissociation rates of $Ca^{2+}$ from the calcium–enzyme complex formed in the presence and absence of ATP were not very different. These results are also consistent with the fact that successful simulations of kinetics of NBD fluorescence change can be carried out by assuming that ATP affects only $k_2$ and the $E_2$ to $E_1$ transition (Table I).

In conclusion, we have presented evidence suggesting that $Ca^{2+}$ binding to the NBD-modified enzyme occurs after the major conformational transition of the enzyme from the state ($E_2$) having low affinity for $Ca^{2+}$ and intermediate affinity for ATP to the one ($E_1$) having high affinity for both $Ca^{2+}$ and ATP. ATP, by binding to a single catalytic site of the $E_2$ form of the free NBD-enzyme prior to $Ca^{2+}$ binding, accelerates the $E_2$ to $E_1$ conversion, thus increasing the overall rate of $Ca^{2+}$ binding and phosphorylation of the enzyme. This mechanism differs from the one proposed previously (Stahl & Jencks, 1986), in which, in the presence of ATP, the enzyme binds $Ca^{2+}$ rapidly without invoking a similar conformational transition.

## Appendix

The interaction of the $Ca^{2+}$-deprived enzyme with ATP is described in Scheme IV (see the text). Assuming rapid association and dissociation of ATP from the enzyme, a relatively rapid transition from the $E_2$ state to the $E_1$ state can be described by the following reduced form:

$$e_1 \underset{k_{-1}}{\overset{k_1}{\rightleftharpoons}} e_2$$

where $e_1 = E_1 + E_1{\cdot}ATP$ and $e_2 = E_2 + E_2{\cdot}ATP$. $k_1$ and $k_{-1}$ can be calculated according to the following equations:

$$k_1 = k'_1\frac{1}{1 + [ATP]/K_2} + k''_1\frac{[ATP]/K_2}{1 + [ATP]/K_2} \quad (1)$$

$$k_{-1} = k'_{-1}\frac{1}{1 + [ATP]/K_1} + k''_{-1}\frac{[ATP]/K_1}{1 + [ATP]/K_1} \quad (2)$$

Thus, the $k_{obs}$ value for the formation of the $E_1$ state, which corresponds to the fast component of the ATP-induced fluorescence rise measured in the absence of $Ca^{2+}$, is given by

$$k_{obs} = k_1 + k_{-1} \quad (3)$$

The ATP concentration at which half-maximal amplitude of the fast component of the ATP-induced fluorescence rise is observed (cf. Figure 7B) is given by the following equation:

$$[ATP]_{1/2} = K_1\frac{1 + k'_{-1}/k'_1}{1 + k''_{-1}/k''_1} = K_2\frac{1 + k'_1/k'_{-1}}{1 + k''_1/k''_{-1}} \quad (4)$$

This equation was formulated on the basis of the equilibrium relationships between the various enzyme species shown in Scheme IV without considering the slow transition from $E_1{\cdot}ATP$ to $E_1{}^*{\cdot}ATP$.

On the other hand, under the equilibrium conditions where the $Ca^{2+}$-deprived enzyme is incubated with ATP, Equation 4 is modified to the following equation, which takes into account the slow transition from $E_1{\cdot}ATP$ to $E_1{}^*{\cdot}ATP$.

$$[ATP]_{1/2} = K_1\frac{1 + k'_{-1}/k'_1}{1 + 1/K_a + k''_{-1}/k''_1} = K_2\frac{1 + k'_1/k'_{-1}}{1 + (1 + K_a)k''_1/k''_{-1}} \quad (5)$$

## References

Andersen, J. P., Jorgensen, P. L., & Moller, J. V. (1985) *Proc. Natl. Acad. Sci. U.S.A. 82*, 4573–4577.

Champeil, P., Gingold, M. P., & Guillain, F. (1983) *J. Biol. Chem. 258*, 4453–4458.

de Meis, L., & de Mello, M. C. F. (1973) *J. Biol. Chem. 248*, 3691–3701.

de Meis, L., & Masuda, H. (1974) *Biochemistry 13*, 2057-2062.
de Meis, L., & Boyer, P. D. (1978) *J. Biol. Chem. 253*, 1556-1559.
de Meis, L., & Vianna, A. L. (1979) *Annu. Rev. Biochem. 48*, 275-292.
Dupont, Y. (1982) *Biochim. Biophys. Acta 688*, 75-87.
Dupont, Y. (1984) *Anal. Biochem. 142*, 504-510.
Dupont, Y., & Leigh, J. B. (1978) *Nature 273*, 396-398.
Fernandez-Belda, F., Kurzmack, M., & Inesi, G. (1984) *J. Biol. Chem. 259*, 9687-9698.
Froud, R. J., & Lee, A. G. (1986) *Biochem. J. 237*, 197-206.
Guillain, F., Gingold, M. P., Büschlen, S., & Champeil, P. (1980) *J. Biol. Chem. 255*, 2072-2076.
Guillain, F., Champeil, P., Lacapere, J.-J., & Gingold, M. P. (1981) *J. Biol. Chem. 256*, 6140-6147.
Guillain, F., Gingold, M. P., & Champeil, P. (1982) *J. Biol. Chem. 257*, 7366-7371.
Ikemoto, N., Morgan, J. F., & Yamada, S. (1978) *J. Biol. Chem. 253*, 8027-8033.
Ikemoto, N., Garcia, A. M., Kurobe, Y., & Scott, T. L. (1981) *J. Biol. Chem. 256*, 8593-8601.
Imamura, Y., Saito, K., & Kawakita, M. (1984) *J. Biochem. (Tokyo) 95*, 1305-1313.
Inesi, G. (1987) *J. Biol. Chem. 262*, 16338-16342.
Inesi, G., Kurzmack, M., Coan, C., & Lewis, D. E. (1980) *J. Biol. Chem. 255*, 3025-3031.
Johnson, R. A., & Walseth, T. F. (1979) *Adv. Cyclic Nucleotide Res. 10*, 135-167.
Martonosi, A., & Beeler, T. J. (1983) *Handb. Physiol. 10*, S417-S485.
Murphy, A. J. (1978) *J. Biol. Chem. 253*, 385-389.
Petithory, J. R., & Jencks, W. P. (1988a) *Biochemistry 27*, 5553-5564.
Petithory, J. R., & Jencks, W. P. (1988b) *Biochemistry 27*, 8626-8635.
Pick, U., & Karlish, S. J. D. (1980) *Biochim. Biophys. Acta 626*, 255-261.
Pick, U., & Karlish, S. J. D. (1982) *J. Biol. Chem. 257*, 6120-6126.
Scofano, H. M., Vieyra, A., & de Meis, L. (1979) *J. Biol. Chem. 254*, 10227-10231.
Shigekawa, M., & Kanazawa, T. (1982) *J. Biol. Chem. 257*, 7657-7665.
Shigekawa, M., Wakabayashi, S., & Nakamura, H. (1983) *J. Biol. Chem. 258*, 8698-8707.
Stahl, N., & Jencks, W. P. (1984) *Biochemistry 23*, 5389-5392.
Stahl, N., & Jencks, W. P. (1987) *Biochemistry 26*, 7654-7667.
Sumida, M., Wang, T., Mandel, F., Froehlich, J. P., & Schwartz, A. (1978) *J. Biol. Chem. 253*, 8772-8777.
Suzuki, H., Obara, M. Kuwayama, H., & Kanazawa, T. (1987) *J. Biol. Chem. 262*, 15448-15456.
Wakabayashi, S., Ogurusu, T., & Shigekawa, M. (1986) *J. Biol. Chem. 261*, 9762-9769.
Wakabayashi, S., Imagawa, T., & Shigekawa, M. (1990) *J. Biochem. (Tokyo) 107*, 563-571.

# A Calcium-Specific Conformational Response of Parvalbumin†

Cindy M. L. Hutnik,‡ John P. MacManus, and Arthur G. Szabo*
*Division of Biological Sciences, National Research Council of Canada, Ottawa, Ontario K1A 0R6, Canada*
*Received October 3, 1989; Revised Manuscript Received April 27, 1990*

ABSTRACT: The single tryptophan containing isotype III parvalbumin from codfish (*Gadus callarius*) was purified by a modified procedure and was shown to be homogeneous by a number of biochemical techniques. Sequence analysis established the location of the single tryptophan in position 102 of the 108 amino acid primary sequence. Atomic absorption spectroscopy showed that trichloroacetic acid (TCA) precipitation was more effective in parvalbumin decalcification compared to the more commonly used method of EGTA treatment. Magnesium induced steady-state fluorescence spectral changes of the EGTA-treated, but not the TCA-treated, parvalbumin. Steady-state fluorescence and circular dichroism spectra showed that calcium, but not magnesium, induced a conformational response in the TCA-treated protein. The fluorescence decay of the calcium-loaded native (holo) cod III parvalbumin was best described by two decay time components. By contrast, three lifetime components were necessary to describe the fluorescence decay of the metal-free (apo) protein. The decay-associated spectra of each temporal component were obtained. Collectively, these results demonstrate that it is possible for a parvalbumin to display a calcium-specific response.

The parvalbumins are low molecular weight (MW ≈12000), acidic, soluble proteins which are ubiquitous in the vertebrate world (Pechère, 1974). On the basis of amino acid sequence data, as well as the X-ray crystallographic structure of carp parvalbumin, these proteins have been found to represent a subfamily of the large superfamily of calcium binding proteins (Kretsinger, 1980). The parvalbumin subfamily is further subdivided based upon two evolutionarily distinct lineages, the α-lineage and the more acidic β-lineage (Goodman & Pechère, 1977).

Over the last 15 years, these proteins and their metal binding properties have been the subject of considerable research. Interpretation of the early thermodynamic and kinetic experiments suggested that the parvalbumins were involved in muscular contraction/relaxation and were $Ca^{2+}/Mg^{2+}$-specific proteins (Pechère et al., 1977; Birdsall et al., 1979). A $Ca^{2+}/Mg^{2+}$-specific protein (1) possesses calcium affinity constants ($K_{Ca}$) on the order of $10^8$–$10^9$ $M^{-1}$ (Moeschler et

† Issued as NRCC Publication No. 31873.
* To whom correspondence should be addressed.
‡ C.M.L.H. is a 1967 NSERC scholar engaged in predoctoral training in the Department of Biochemistry, University of Ottawa, working under the supervision of A.G.S. at the NRCC.

0006-2960/90/0429-7318$02.50/0 